

Behavioral experiments for understanding catastrophic forgetting

Samuel J. Bell Neil D. Lawrence
 Dept. of Computer Science & Technology,
 University of Cambridge,
 United Kingdom
 {sjb326,nd121}@cam.ac.uk

Abstract

In this paper we explore whether the fundamental tool of experimental psychology, the behavioral experiment, has the power to generate insight not only into humans and animals, but artificial systems too. We apply the techniques of experimental psychology to investigating catastrophic forgetting in neural networks. We present a series of controlled experiments with two-layer ReLU networks, and exploratory results revealing a new understanding of the behavior of catastrophic forgetting. Alongside our empirical findings, we demonstrate an alternative, behavior-first approach to investigating neural network phenomena.

1 Introduction

In a parallel universe, scientists discover *R. Obliviosus*, a new species of rat that forgets something old each time it learns something new. This behavior provokes significant intrigue, raising such questions as when does this new rat forget, what does it forget, and why? Faced with such a surprising phenomenon, one might look to the experimental psychologist for answers. Through the careful design of controlled behavioral experiments, the psychologist seeks to observe and explain the rat’s forgetfulness. The psychologist’s experiments can be remarkably informative, even enabling a step beyond surface behavior, and towards an understanding of unseen and underlying processes.¹

In this universe, our *R. Obliviosus* is the two-layer ReLU network, and—like neural networks more broadly—it too suffers from catastrophic forgetting (CF). CF, where training on a new task results in degraded performance on a previously learned task, remains a fundamental issue that pervades the study and application of neural networks (McCloskey and Cohen 1989; Ratcliff 1990; French 1999; Parisi et al. 2019; Hadsell et al. 2020). The often dramatic decline

¹For an insightful series of examples see Niv (2021).

in previous task performance, while the subject of numerous studies, is still only partially understood both empirically and theoretically.

The human experiments of Kattner et al. (2017), investigating perceptual learning transfer, perfectly illustrate our approach. Perceptual learning is developing increased sensitivity to sensory information through experience (Fahle and Poggio 2002). Across many perceptual tasks, a wide array of evidence indicates that performance improvement is *specific* (Fiorentini and Berardi 1980; Karni and Sagi 1991; Poggio et al. 1992), i.e. it does not *transfer* to other settings, such as a rotation of the stimuli through 90° (Fiorentini and Berardi 1980), or a switch from one eye to the other (Fahle 2004).²

Among humans, transfer is typically measured by performance improvement on task B after training on a previous task A, without any training on B. Challenging this approach, Kattner et al. train their human participants on contrasting sequences of tasks, each sequence unique in the way their constituent tasks differ. Arguing that measuring *point-in-time* performance obscures transfer, Kattner et al. show that training on similar tasks induces an increase in learning *rate*, even when immediate performance change isn't apparent. In a related study (Kattner et al. 2016), the authors again compare different types of task similarity, though here identifying that tasks that share a similar underlying structure exhibit greater transfer, even when their surface forms are radically different.

Both of these studies *begin* with experiments designed to isolate behavior in specific circumstances, and proceed to drawing conclusions from the resulting observations. Also starting with behavior, we attempt to follow in the footsteps of the psychologist, exploring how simple behavioral experiments can shed light onto the phenomenon of CF. Like Kattner et al., we experiment with sequences of visual classification tasks and manipulate the dimensions of task similarity, though rather than perceptual learning our goal is to understand CF. Our results indicate that CF is situation-specific, reveal the differential effects of perceptual and semantic task similarity, and demonstrate that the new task's loss surface is associated with forgetting. Equipped with a sample of trained models, we investigate how their parameters have changed through time, and as a result identify a simple heuristic based on the gradients of the new task's loss function—after just a single backward pass—that is strongly predictive of CF. Finally, we validate our findings on a different dataset, a randomized version of split-MNIST (LeCun et al. 2010; Zenke et al. 2017).

²Monocular specificity is indeed a wonderful example of behavior informing understanding of internal process: combined with knowledge of cortical anatomy, it provided early evidence of the role played by orientation-selective cells (Fahle 1994), well before these results were confirmed in electrophysiological (Schoups et al. 2001) and neuroimaging studies (Furmanski et al. 2004).

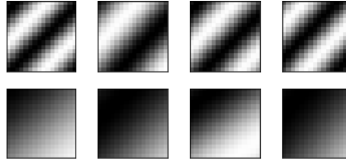


Figure 1: Image samples from a binary classification task over sinusoidal gratings. **Top:** Category 0. **Bottom:** Category 1.

2 Related work

2.1 Connectionism

There is a long tradition of connectionist investigations into CF (McCloskey and Cohen 1989; Ratcliff 1990; French 1993; Robins 1995; French 1999). While we have an empirical focus in common, our aims, however, fundamentally differ: rather than investigating neural networks in search of psychological plausibility, here we use the *methods* of psychology to investigate neural networks. We make no claim as to the status of the neural network as model of mind or brain, we only suggest that the behavior-first approach is a useful experimental paradigm.

Often using two-layer neural networks, connectionists probing CF have produced various theories as to its cause, including that representational overlap between tasks drives CF (French 1993); that backpropagation overwrites what were previously the most important weights first (Sutton 1986); and that rehearsal of previous tasks can help to mitigate CF (Robins 1995). These investigations involved small amounts of low-dimensional and noiseless data, which is an unrealistic setting for contemporary machine learning practice. While we also study a two-layer non-linear network, our models are trained with stochastic gradient descent, i.e. gradients averaged over a random batch, rather than online after each training example.

2.2 Empirical investigations

We are by no means the first to conduct empirical research into CF. More recent investigation has involved analysis of the effect of hyperparameters (Goodfellow et al. 2014); mitigation strategies (Kemker et al. 2018); and benchmark datasets (Zenke et al. 2017; Ramasesh et al. 2020). Unlike previous work, however, we apply our *psychological* ethos through the development of new tasks tailored to investigating CF. In contrast, experiments with split/permuted MNIST/CIFAR, while useful for model comparison, tell us little about the circumstances under which CF may take place, given the difficulty of precisely quantifying similarity between tasks.³ Ramasesh et al. (2020) investigate learned representations across tasks, distinguishing between surface form and semantic similarity, and

³For example, is a 0 vs. 1 digit classification more or less similar to 2 vs. 3 than to 4 vs. 5? In which ways are these tasks similar, and how do they differ?

suggesting evidence that moving between semantically-similar tasks leads to less CF. We follow this line of investigation into semantic and perceptual differences, though use synthetic data to precisely control task similarity.

Lee et al. (2021) outline both empirical experiments in a teacher-student setup and an analytical account of continual learning dynamics. The authors disentangle “feature-level” from “readout-level” task similarity (i.e. perceptual from semantic), defined as the teacher-student overlap in the input (“feature”) and output (“readout”) layer weights. Our experiments are designed to take these distinct notions of similarity and translate them into new datasets of noisy, high-dimensional images that more closely approximate a real deep learning setting.

2.3 Mitigation attempts

A significant body of research tries to mitigate the effects of CF, falling broadly into regularization strategies (French 1993; Kirkpatrick et al. 2017; Zenke et al. 2017; Li and Hoiem 2018); capacity allocation (Goodrich and Arel 2014), and rehearsal or replay (Robins 1995; French and Chater 2002). As our study investigates the behavioral phenomenon of CF, we do not present a detailed survey of such work. We do however highlight the similarity of our gradient-based heuristic to the regularizing term of Kirkpatrick et al. (2017), whose *Elastic Weight Consolidation* also makes use of the diagonal of the Fisher information matrix to approximate the Hessian of the loss surface. Mirzadeh et al. (2020) also investigate the curvature of the first task loss, testing hyperparameter combinations that should lead to minima with wider curvature, and hence mitigate CF when tested on split/rotated MNIST and CIFAR-10. Our work—as described in section 3.5—differs in its focus on the new task loss surface, rather than the former.

3 Methods

We now describe our four behavioral experiments designed to investigate CF. Each experiment involves different types of “curricula”: sequences of tasks that differ in various ways. After training two-layer ReLU networks on these curricula, we analyze the resulting network behavior by measuring validation losses. Starting with our behavioral results, and a population of models to match, we then analyze parameter change throughout training on each task, and the associated loss function gradients.

For a formal definition, given two tasks \mathcal{T}_j and \mathcal{T}_{j+1} , let \mathcal{M}_θ be a parameterized model to be sequentially trained on both tasks. We denote the model’s parameters after training on task j and $j + 1$ as θ_j and θ_{j+1} respectively. Assuming our model is optimized to minimize some loss function for each task

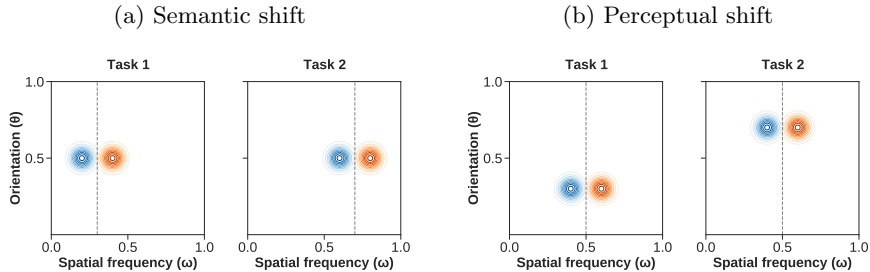


Figure 2: Illustration of contrasting curricula of binary classification tasks (blue vs. orange). All categories are separable by ω ; decision boundary is dashed gray line. **(a)** Tasks in curriculum \mathcal{C}_S differ semantically: the decision boundary shifts from task to task. **(b)** Tasks in \mathcal{C}_P are semantically similar and share a decision boundary, yet differ perceptually due to varying θ .

$L_j(\boldsymbol{\theta}) \in \mathbb{R}$, we define CF as a function of the two tasks:

$$F(\mathcal{T}_j, \mathcal{T}_{j+1}) = \begin{cases} 1 & \text{if } L_j(\boldsymbol{\theta}_{j+1}) - L_j(\boldsymbol{\theta}_j) > \epsilon \\ 0 & \text{otherwise,} \end{cases}$$

where ϵ is some acceptable threshold. Thus, we test for CF by training a model on task \mathcal{T}_j followed by \mathcal{T}_{j+1} . Then, without updating its parameters, we re-evaluate performance of the trained model on the original task \mathcal{T}_j . This sequential training approach forms the basis of this work.

3.1 Gratings experiments

Kattner et al. (2017) investigate human transfer learning using sequences of classification tasks, where each task comprises linearly-separable categories defined by 2D Gaussians. In our first three experiments, we follow this approach, defining a curriculum \mathcal{C} as a set of tasks,

$$\mathcal{C} = \{ \mathcal{T}_j \mid 1 \leq j \leq N \},$$

where each task \mathcal{T}_j is a pair of 2D Gaussian distributions for its two categories,

$$\mathcal{T}_j = \{ \mathcal{N}(\boldsymbol{\mu}_j, \boldsymbol{\Sigma}), \mathcal{N}(\boldsymbol{v}_j, \boldsymbol{\Sigma}) \}.$$

with each category parameterized by its mean vector $\boldsymbol{\mu}_j$ or \boldsymbol{v}_j and covariance matrix $\boldsymbol{\Sigma} = I$. We manipulate and explore task similarity through modifying the difference between mean vectors.

3.1.1 Grating classification task setup

Tasks in experiments 1 to 3 are a binary classification of sinusoidal gratings, with each grating defined by its orientation in radians θ , spatial frequency (s.f.)

ω , and phase ϕ . To set these parameters, $[\omega, \theta]$ are drawn from the task category distributions \mathcal{T} , though ϕ varies randomly across all tasks. Across all curricula, success requires classifying gratings according to their s.f., invariant to orientation and phase. See fig. 1 for an example.

For each task, we first draw $n = 1,000$ category labels $\mathbf{y} \in \mathbb{B}^n$ from a Bernoulli distribution, before drawing parameters for the images themselves from their corresponding category distribution \mathcal{T}_j ,

$$\begin{aligned} \mathbf{y} = \mathbf{y}_i &\sim \text{Bern}(0.5) \\ [\omega_i, \theta_i]^\top &\sim \mathcal{T}_{j,y}. \end{aligned}$$

Equipped with ω_i and θ_i , the sampled image in terms of its pixel luminosity l (for all pixels x and y) is, following (Goodfellow et al. 2012),

$$\begin{aligned} \mathbf{x}_i &= [l(0,0), \dots, l(15,15)]^\top, \\ l(x,y) &= \sin(\omega_i(x \cos(\theta_i) + y \sin(\theta_i) - \phi_i)), \end{aligned}$$

where $\phi_i \sim \mathcal{U}(0,1)$. Due to ϕ , $l(\cdot)$ is an embedding from the low-dimensional latent task space to noisy, high-dimensional image space. Thus, by manipulating the parameters of the tasks' category distributions, we control latent task similarity.

3.1.2 Experiment 1: Contrasting curricula

In our first behavioral experiment, we contrast two different three-task ($N = 3$) curricula. Both curricula are identical but for the dimension of $\boldsymbol{\mu}$ that varies between tasks. In the semantic-shift condition, \mathcal{C}_S , the s.f. dimension of the mean vector varies but the orientation remains fixed. Conversely, in the perceptual-shift condition \mathcal{C}_P , the s.f. dimension has fixed mean but the orientation varies.

As categories are always ω -separable, \mathcal{C}_S requires learning a new separating plane for each task, without forgetting previous category boundaries. In contrast, learning \mathcal{C}_P only requires learning a single category boundary, though invariant to changes in θ between tasks. See fig. 2 for example category distributions.

3.1.3 Experiments 2 and 3: Randomized curricula

Our second and third behavioral experiments introduce the random task paradigm. Here we generate random curricula, \mathcal{C}_{Ri} , comprising pairs of random tasks \mathcal{T}_{Rj} :

$$\begin{aligned} \mathcal{C}_{Ri} &= \{ \mathcal{T}_{R1}, \mathcal{T}_{R2} \}, \quad 1 \leq i \leq 30 \\ \mathcal{T}_{Rj} &= \{ \mathcal{N}(\boldsymbol{\mu}_j, \boldsymbol{\Sigma}), \mathcal{N}(\mathbf{v}_j, \boldsymbol{\Sigma}) \} \end{aligned}$$

The mean vectors for the first task \mathcal{T}_{R1} are drawn from a 2D uniform distribution across latent feature space,

$$\boldsymbol{\mu}_1 \in \mathcal{U}(0.2, 0.8) \quad \text{and} \quad \mathbf{v}_1 = \boldsymbol{\mu}_1 + \mathbf{c},$$

where $\mathbf{c} = [0.2, 0]^\top$ is a fixed vector defining category separation. The second task \mathcal{T}_{R2} is a modification of the first task by \mathbf{d}_i ,

$$\mathbf{d}_i = \mathcal{U}(-1, 1), \quad \hat{\mathbf{d}}_i = \frac{\mathbf{d}_i}{|\mathbf{d}_i|},$$

$$\boldsymbol{\mu}_2 = \boldsymbol{\mu}_1 + \gamma \hat{\mathbf{d}}_i \quad \text{and} \quad \mathbf{v}_2 = \mathbf{v}_1 + \gamma \hat{\mathbf{d}}_i,$$

where $\gamma = 0.25$ is a scaling constant that fixes the distance between tasks (see appendix D for different choices of γ). According to \mathbf{c} and γ , both the inter-task and inter-category distances are held constant. Unlike experiment 1, task pairs can differ in both the semantic and perceptual dimensions, depending on the direction of \mathbf{d}_i . In experiment 2, the first task is held constant and the second task is randomized. In experiment 3, both tasks are drawn at random.

3.2 Experiment 4: Randomized MNIST curricula

Our fourth experiment tests the validity of our findings outside the gratings task. We turn to a randomized variant of split-MNIST (Zenke et al. 2017):

$$\mathcal{C}_{Mi} = \{ \mathcal{T}_{M1}, \mathcal{T}_{M2} \}, \quad 1 \leq i \leq 30$$

$$\mathcal{T}_{Mj} = \{ (X_{j0}, y_{j0}), (X_{j1}, y_{j1}) \},$$

where y_{j0}, y_{j1} are sampled without replacement from the class labels $\{0, \dots, 9\}$, and X_{j0}, X_{j1} are the corresponding inputs. For consistency with experiments 1–3, input images are resized to 16×16 pixels using bilinear interpolation. The first task in every curriculum is a binary classification of a random pair of digits, and the second task is another random pair. See appendix A for full task parameters for all four experiments.

3.3 Model architecture

All experiments are performed on two-layer ReLU networks. Let $\mathbf{x} \in \mathbb{R}^d$ be an input vector representing an image, and let $W_1 \in \mathbb{R}^{d \times h}$, $W_2 \in \mathbb{R}^{h \times 1}$ and $\mathbf{b}_1 \in \mathbb{R}^h$, $\mathbf{b}_2 \in \mathbb{R}^1$ be the weights and biases for the first and second layers. Then, the network’s decision $\hat{y} \in \mathbb{R}$ is

$$\hat{y} = s(W_2^\top \mathbf{a} + \mathbf{b}_2), \quad \mathbf{a} = r(W_1^\top \mathbf{x} + \mathbf{b}_1),$$

where

$$r(x) = \max(0, x), \quad s(x) = \frac{1}{1 + e^{-x}},$$

i.e. $r(\cdot)$ and $s(\cdot)$ are the element-wise ReLU and sigmoid functions respectively. For our specific networks, $d = h = 256$, and batch normalization is used to center and scale the inputs to have zero mean and unit variance.⁴

⁴We make available all models, datasets, results and code from this work.

3.4 Model training

Model training is the same across all curricula in all experiments unless otherwise noted. Network weights and biases are randomly initialized from $\mathcal{U}(-\sqrt{d}, \sqrt{d})$ at the start of each curriculum, and for subsequent tasks model parameters for task j are initialized to $\boldsymbol{\theta}_{j-1}$. The network is then trained sequentially on each task, using batches of 128 images, for 1,000 epochs in experiments 1-3 and 5,000 epochs in experiment 4. Networks are trained to minimize the cross-entropy loss using vanilla stochastic gradient descent with learning rate 0.001, with neither learning rate decay nor explicit regularization penalties. 10 models with different random seeds are trained for each experimental condition. Number of epochs and learning rate were manually set according to pilot experiments. No other model or optimization hyperparameters were tuned, though see appendices B and C for a post-hoc analysis of the effect of learning rate and weight decay.

3.5 Loss surface analysis

Using the population of models trained in our behavioral experiments, we now investigate the loss function gradients with the goal of identifying how they relate to CF. Mirzadeh et al. (2020) argues that the curvature of $L_j(\boldsymbol{\theta}_j)$ determines forgetting, loosely bounding the change in first task loss between $\boldsymbol{\theta}_j$ and $\boldsymbol{\theta}_{j+1}$ by the spectral radius of the Hessian of the first task loss. In section 4.3 we present behavioral evidence that this is not the case, and show that from a constant first task (i.e. assuming a constant minima) CF varies significantly depending on the choice of *second* task. Instead, we suggest that the first gradient update of the *new* task explains CF.

Like Mirzadeh et al., we approximate the loss surface in with a second-order Taylor expansion, though we focus on L_{j+1} rather than L_j :

$$L_{j+1}(\boldsymbol{\theta}_j + \epsilon \mathbf{g}) = L_{j+1}(\boldsymbol{\theta}_j) + \epsilon \mathbf{g}^\top \mathbf{g} + \frac{1}{2} \epsilon^2 \mathbf{g}^\top H \mathbf{g}, \quad (1)$$

where $\mathbf{g} = \nabla_{\boldsymbol{\theta}_j} L_{j+1}(\boldsymbol{\theta}_j)$ is the gradient and $H = \nabla_{\boldsymbol{\theta}_j}^2 L_{j+1}(\boldsymbol{\theta}_j)$ is the Hessian matrix around $\boldsymbol{\theta}_j$, the collection of $(W_1, W_2, \mathbf{b}_1, \mathbf{b}_2)$ after training on task j .

We note that most prior work makes use of the difference between the post-training minima of the two tasks, predicating analysis on completing second task training before determining whether CF will occur. In contrast, using experiments 3 and 4, we show that a single gradient update—calculated using a single backward pass—is sufficient. From eq. (1), the change in loss is determined by the norm of the gradient ($\mathbf{g}^\top \mathbf{g}$), corrected for curvature ($\mathbf{g}^\top H \mathbf{g}$). As computing H is impractical for a large number of parameters, we crudely approximate H using the diagonal of the empirical Fisher information matrix (Ritter et al. 2018;

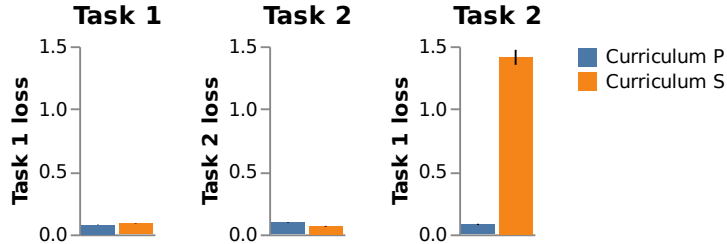


Figure 3: **Experiment 1. Left:** Mean task 1 validation loss after training on task 1. **Middle:** Task 2 validation loss after training on task 1 and task 2. **Right:** Task 1 validation loss after training on task 1 and 2. Only semantic-shift curriculum \mathcal{C}_S (orange) exhibits CF. Error bars are standard deviation.

Immer et al. 2021; Kirkpatrick et al. 2017),

$$\begin{aligned}
 H &\approx F = \sum_i \nabla_{\theta_j} (\log P(y_i | \mathbf{x}_i; \boldsymbol{\theta}_j)) (\log P(y_i | \mathbf{x}_i; \boldsymbol{\theta}_j))^\top \\
 &= \mathbf{g} \mathbf{g}^\top \\
 &\approx \text{Diag}(\text{diag}(\mathbf{g} \mathbf{g}^\top)) \\
 &= \text{Diag}(\mathbf{g}^2)
 \end{aligned}$$

where $\text{Diag}(\mathbf{v})$ returns a diagonal matrix, and $\text{diag}(M)$ returns its diagonal elements. As such we roughly approximate the dominant eigenvalue of H with $\|\mathbf{g}^2\|_\infty$, providing an alternative to the λ_{max} bound of Mirzadeh et al. In section 4.5, we show that even the first step away from $\boldsymbol{\theta}_j$ determines CF, and as such $\|\mathbf{g}\|_\infty$ is strongly correlated with future forgetting.

4 Results

4.1 Semantic task difference drives CF

Experiment 1 demonstrates that CF only occurs in certain situations (fig. 3). In both the semantic-shift (\mathcal{C}_S) and perceptual-shift (\mathcal{C}_P) conditions, models learn to perform each task, achieving validation loss $L_1(\boldsymbol{\theta}_1)$ of 0.087 ± 0.002 (mean \pm SD) and 0.076 ± 0.002 for \mathcal{C}_S and \mathcal{C}_P respectively, and $L_2(\boldsymbol{\theta}_2)$ of 0.064 ± 0.004 and 0.094 ± 0.003 . CF is selectively apparent, with $L_1(\boldsymbol{\theta}_2)$ rising significantly to 1.412 ± 0.060 for \mathcal{C}_S and remaining at 0.079 ± 0.005 for \mathcal{C}_P ($t(18) = 70.18$, $p < .0001$, Welch’s t -test for unequal variances). This result suggests that CF is most significant when tasks are perceptually similar but vary in their semantic mapping, and conversely that semantically-similar tasks that only vary perceptually are less likely to induce CF, aligning with results presented by Ramasesh et al. (2020) and Lee et al. (2021).

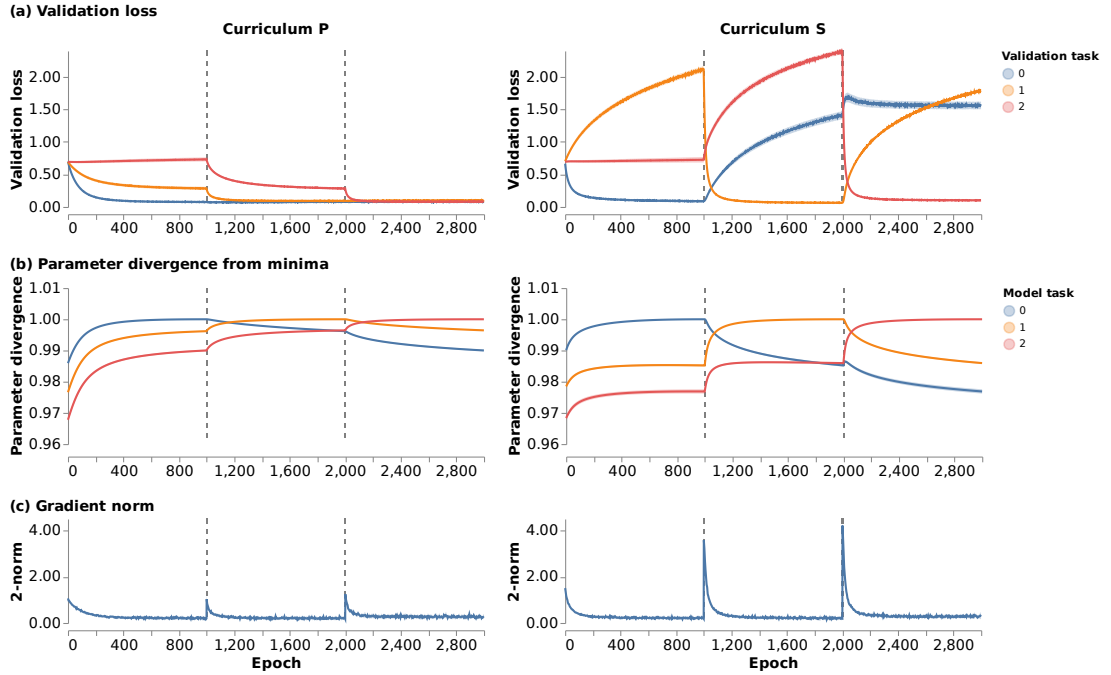


Figure 4: **Experiment 1. Left: \mathcal{C}_P . Right: \mathcal{C}_S .** (a) Mean validation loss for all three tasks with sequential training from task to task. Grey dashed lines indicate task change. Only \mathcal{C}_S exhibits CF. (b) Dot product of model parameters at each epoch and at minima for each task. Parameters sharply diverge from minima in \mathcal{C}_S . (c) 2-norm of gradient of training loss w.r.t. all parameters. Larger gradient updates take place in \mathcal{C}_S . Shaded region (barely visible) is standard deviation.

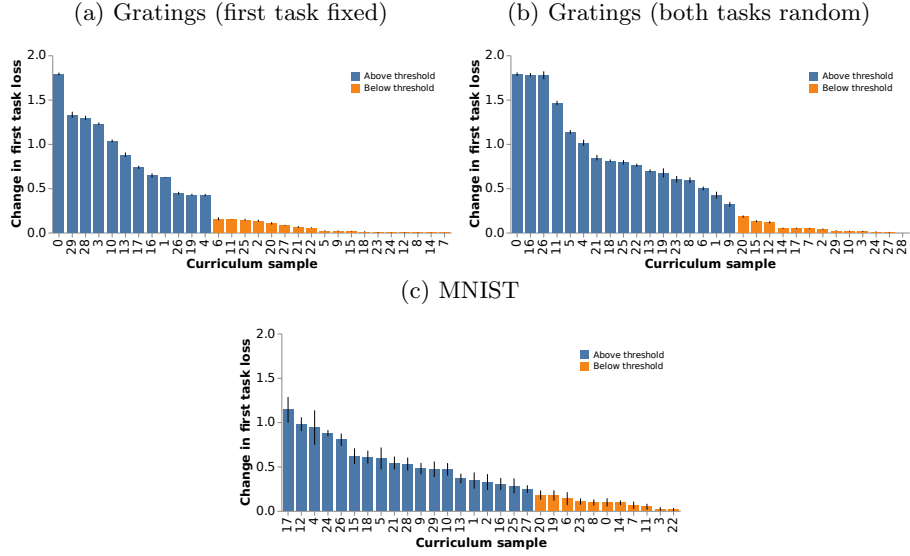


Figure 5: **Experiments 2–4:** Change in mean first task validation loss after training on second task over curricula of (a) gratings, first task fixed and second randomized; (b) gratings, both tasks randomized; (c) split MNIST, both tasks randomized. Only certain curricula exhibit forgetting in all experiments. Error bars are standard deviation.

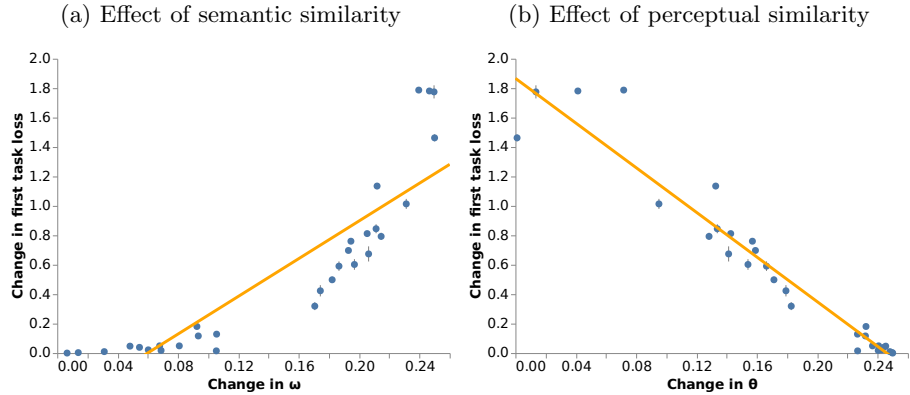


Figure 6: **Experiment 3.** Effect of change in θ and ω on first task loss. (a) Increased semantic distance (change in ω) leads to greater CF. (b) Increased perceptual distance (change in θ) leads to reduced CF. Orange regression line is for illustration only, see main text for Pearson’s r . Error bars are standard deviation.

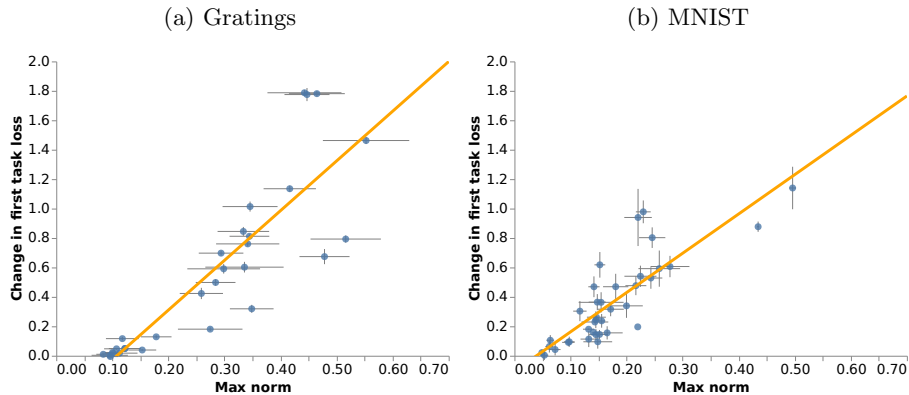


Figure 7: **Experiments 3 and 4:** Change in first task loss and ∞ -norm of gradient of second task training loss after single pass on second task. In both (a) randomized curricula and (b) split MNIST the ∞ -norm is strongly positively and highly significantly correlated with CF. Orange regression line is for illustration only, see main text for Pearson’s r . Error bars are standard deviation.

4.2 Parameter dynamics mirror CF

Figure 4a shows the validation losses for each task in both curricula of experiment 1 over time. In both curricula, as training on the j th task commences, $L_j(\cdot)$ decreases until converging to its minimum. In curriculum \mathcal{C}_P , once a model has reached its minimum loss for task j , it is maintained for all tasks $k > j$. In curriculum \mathcal{C}_S , however, loss $L_j(\cdot)$ sharply increases as soon as training progresses onto subsequent tasks $k > j$.

These dynamics are broadly mirrored by network parameter change as training progresses across tasks. Figure 4b shows the deviation of the parameters at time t from the minima reached at the end of training on task j , i.e. $\theta_j^\top \theta(t)$. In \mathcal{C}_S , parameters move rapidly away from their minima as training crosses the task boundary.

Figure 4c shows the 2-norm of the gradient vector through training across tasks, demonstrating much sharper peaks at the task boundaries in \mathcal{C}_S than \mathcal{C}_P . In section 4.5, we show that the size of this first update after the boundary is predictive of CF.

4.3 First task curvature

Mirzadeh et al. (2020) argue that the curvature of the first task loss surface around the achieved minima is responsible for forgetting, suggesting that a shallower curvature leads to less forgetting and a steeper curvature to more. In experiment 2, we hold the first task constant and randomly vary the second task, yielding 30 different curricula. Figure 5a shows that from this constant

first task, using a threshold of $\epsilon = 0.2$, some curricula result in CF (12/30) and others do not (18/30), with first task loss $L_1(\boldsymbol{\theta}_2)$ ranging from 0.063 to 1.891. We assume that as we hold the first task, and hence its loss function, fixed, that the curvature of the obtained minima is also constant. Thus, from a simple behavioral experiment, we conclude that first task curvature cannot explain forgetting.

4.4 Random curricula

In experiment 3, all models successfully learn to perform both tasks in order, with $L_1(\boldsymbol{\theta}_1) = 0.075 \pm 0.011$ and $L_2(\boldsymbol{\theta}_2) = 0.069 \pm 0.015$. After training on the second task, first task loss $L_1(\boldsymbol{\theta}_2)$ rises to 0.631 ± 0.567 , with one model reaching a minimum loss of 0.052 and another reaching a maximum of 1.921. As with experiment 2, only certain task pairs (17/30) induce CF (fig. 5b).

Figure 6 shows the effect of task distance along either the semantic or perceptual dimension. As with experiment 1, a semantic shift between tasks is associated with increased CF (Pearson’s $r(28) = -0.97$, $p < .0001$), whereas a perceptual shift is associated with a decrease ($r(28) = 0.88$, $p < .0001$).

We see similar results in experiment 4. Here, all models successfully learn both tasks, reaching $L_1(\boldsymbol{\theta}_1) = 0.062 \pm 0.032$ and $L_2(\boldsymbol{\theta}_2) = 0.067 \pm 0.034$. First task loss after training on task 2 is $L_1(\boldsymbol{\theta}_2) = 0.565 \pm 0.758$, with a minimum of 0.006 and a maximum of 3.905, and 18/30 curricula exhibiting forgetting (fig. 5c).

4.5 First update gradient norm predicts CF

Following section 3.5, we present evidence that the max-norm of the first gradient step of the *new* task, $\|\nabla_{\theta_j} L_{j+1}(\boldsymbol{\theta}_j)\|_\infty$, is predictive of forgetting. For both experiments 3 and 4, over gratings and split MNIST respectively (see fig. 7), the change in first task loss is strongly positively and highly significantly correlated with the max-norm of the new task first gradient step (experiment 3: Pearson’s $r(28) = 0.87$, $p < .0001$; experiment 4: $r(28) = 0.83$, $p < .0001$). Supporting our choice of focus on the new task, the max norm of an additional gradient step minimizing the original loss, $\|\nabla_{\theta_j} L_j(\boldsymbol{\theta}_j)\|_\infty$, is uncorrelated with the change in loss (experiment 3: $r(28) = -0.01$, $p = .96$; experiment 4: $r(28) = 0.04$, $p = .82$).

5 Discussion

This exploratory study demonstrates how carefully-designed behavioral experiments can elucidate the surprising phenomena that neural networks exhibit. In this work, our chosen phenomenon is catastrophic forgetting, and through our experiments we have presented a number of behavioral findings. First, we have shown that CF is associated more with semantic-level than perceptual task differences, aligning our results with those of Ramasesh et al. (2020) and Lee et al.

(2021). Second, we have challenged the view that the loss surface of the first task is responsible for CF, in contrast to the focus of Mirzadeh et al. (2020) and Kirkpatrick et al. (2017). Beyond behavior, we have analyzed the parameters of our model population, presenting evidence that parameter divergence from the task minima tracks increase in loss. Finally, our results have led us to a simple and easy-to-compute heuristic, the max-norm of the first gradient step, that can immediately predict the occurrence of CF.

While we have validated our findings against the randomised split-MNIST, future work should confirm that these results indeed hold in more general settings. We argue that a tailor-made task can be far more informative than a general-purpose vision dataset, and so advocate first for behavioral experiments, and later for validation in challenging and large-scale continual learning environments. Similarly, in this work we have studied two-layer ReLU networks, though a clear path forward is to investigate how our findings generalize to the multi-layer networks in common use. Just as one might study an animal (*R. Obliviosus*) as a model organism for a different species, so too can our two-layer networks generate insight about more complex models.

Regarding such complex models, a key theme of contemporary deep learning is overparameterization. It seems probable that network capacity plays some role in determining task similarity: we intuitively expect that a larger network could learn a greater number of tasks without suffering CF. Given the surprising absence of overfitting in overparameterized networks, we suggest further investigation of the relationship between the “double-dip” phenomenon (Belkin et al. 2019) and CF. Double-dip studies have to-date studied generalization to out-of-sample distributions, that is, to unseen distributions that are assumed to be similar to the training distribution. A natural extension to this line of inquiry is to consider the intentionally *different* distributions of a multi-task setting.

Making use of our gradient norm heuristic, future work could look to modify gradient descent to update parameters while causing the least disruption to initial task performance. We see this as potentially manifesting in regularizers that prevent CF, or new optimization mechanisms designed specifically for continual learning. For example, given a choice of equally-good (in terms of generalization error) minima for some initial task, our heuristic could perhaps identify those that will lead to the least CF after subsequent training.

6 Concluding remarks

We hope that our approach—starting with task design specifically to tease apart behavior, before moving on to internals—proves a thought-provoking inspiration for future research. Where the tools of fields such as statistical mechanics allow for reasoning about the state of a system from the states of its parts, the tools of experimental psychology enable the opposite. We can not only observe and catalog a system’s behaviors, but with the right experiments we can unpick how they arose, even without full knowledge of the relation between internal gener-

ative process and emergent phenomenon (Bell and Kampman 2021). Though our subjects are neural networks rather than humans or animals, the powerful empirical techniques given to us by over a century of experimental psychologists await their new applications.

References

- Belkin, M., Hsu, D., Ma, S., and Mandal, S. (2019). “Reconciling modern machine-learning practice and the classical bias–variance trade-off”. In: *Proceedings of the National Academy of Sciences of the United States of America* 116.32, pp. 15849–15854. DOI: 10.1073/pnas.1903070116.
- Bell, S. J. and Kampman, O. P. (2021). *Perspectives on machine learning from psychology’s reproducibility crisis*. arXiv: 2104.08878 [cs.LG].
- Fahle, M. (1994). “Human pattern recognition: parallel processing and perceptual learning”. In: *Perception* 23.4, pp. 411–427. DOI: 10.1068/p230411.
- Fahle, M. (2004). “Perceptual learning: a case for early selection”. In: *Journal of Vision* 4.10, pp. 879–890. DOI: 10.1167/4.10.4.
- Fahle, M. and Poggio, T. (2002). *Perceptual Learning*. MIT Press. Chap. 1.
- Fiorentini, A. and Berardi, N. (1980). “Perceptual learning specific for orientation and spatial frequency”. In: *Nature* 287.5777, pp. 43–44. DOI: 10.1038/287043a0.
- French, R. M. (1993). “Using semi-distributed representations to overcome catastrophic forgetting in connectionist networks”. In: *Proceedings of the AAAI Spring Symposium*. 1993, pp. 70–77.
- French, R. M. (1999). “Catastrophic forgetting in connectionist networks”. In: *Trends in Cognitive Sciences* 3.4, pp. 128–135. DOI: 10.1016/S1364-6613(99)01294-2.
- French, R. M. and Chater, N. (2002). “Using noise to compute error surfaces in connectionist networks: a novel means of reducing catastrophic forgetting”. In: *Neural Computation* 14.7, pp. 1755–1769. DOI: 10.1162/08997660260028700.
- Furmanski, C. S., Schluppeck, D., and Engel, S. A. (2004). “Learning strengthens the response of primary visual cortex to simple patterns”. In: *Current Biology* 14.7, pp. 573–578. DOI: 10.1016/j.cub.2004.03.032.
- Goodfellow, I. J., Le, Q. V., Saxe, A. M., Lee, H., and Ng, A. Y. (2012). “Measuring invariances in deep networks”. In: *Advances in Neural Information Processing Systems*. Vol. 22, pp. 646–654.
- Goodfellow, I. J., Mirza, M., Xiao, D., Courville, A., and Bengio, Y. (2014). “An empirical investigation of catastrophic forgetting in gradient-based neural networks”. In: *2nd International Conference on Learning Representations, ICLR 2014, Conference Track Proceedings*.
- Goodrich, B. and Arel, I. (2014). “Unsupervised neuron selection for mitigating catastrophic forgetting in neural networks”. In: *Proceedings of the 57th IEEE International Midwest Symposium on Circuits and Systems*, pp. 997–1000. DOI: 10.1109/MWSCAS.2014.6908585.

- Hadsell, R., Rao, D., Rusu, A. A., and Pascanu, R. (2020). “Embracing change: continual learning in deep neural networks”. In: *Trends in Cognitive Sciences* 24.12, pp. 1028–1040. DOI: 10.1016/j.tics.2020.09.004.
- Immer, A., Bauer, M., Fortuin, V., Rätsch, G., and Khan, M. E. (2021). *Scalable marginal likelihood estimation for model selection in deep learning*. arXiv: 2104.04975 [stat.ML].
- Karni, A. and Sagi, D. (1991). “Where practice makes perfect in texture discrimination: evidence for primary visual cortex plasticity”. In: *Proceedings of the National Academy of Sciences of the United States of America* 88.11, pp. 4966–4970. DOI: 10.1073/pnas.88.11.4966.
- Kattner, F., Cochrane, A., Cox, C. R., Gorman, T. E., and Green, C. S. (2017). “Perceptual learning generalization from sequential perceptual training as a change in learning rate”. In: *Current Biology* 27.6, pp. 840–846. DOI: 10.1016/j.cub.2017.01.046.
- Kattner, F., Cox, C. R., and Green, C. S. (2016). “Transfer in rule-based category learning depends on the training task”. In: *PLoS ONE* 11.10, pp. 1–17. DOI: 10.1371/journal.pone.0165260.
- Kemker, R., McClure, M., Abitino, A., Hayes, T. L., and Kanan, C. (2018). “Measuring catastrophic forgetting in neural networks”. In: *Proceedings of the 32nd AAAI Conference on Artificial Intelligence*, pp. 3390–3398.
- Kirkpatrick, J., Pascanu, R., Rabinowitz, N., Veness, J., Desjardins, G., Rusu, A. A., Milan, K., Quan, J., Ramalho, T., Grabska-Barwinska, A., Hassabis, D., Clopath, C., Kumaran, D., and Hadsell, R. (2017). “Overcoming catastrophic forgetting in neural networks”. In: *Proceedings of the National Academy of Sciences of the United States of America* 114.13, pp. 3521–3526. DOI: 10.1073/pnas.1611835114.
- LeCun, Y., Cortes, C., and Burges, C. (2010). *MNIST handwritten digit database*.
- Lee, S., Goldt, S., and Saxe, A. (2021). “Continual learning in the teacher-student setup: impact of task similarity”. In: *Proceedings of the 38th International Conference on Machine Learning*. Vol. 139. Proceedings of Machine Learning Research, pp. 6109–6119.
- Li, Z. and Hoiem, D. (2018). “Learning without forgetting”. In: *IEEE Transactions on Pattern Analysis and Machine Intelligence* 40.12, pp. 2935–2947. DOI: 10.1109/TPAMI.2017.2773081.
- McCloskey, M. and Cohen, N. J. (1989). “Catastrophic interference in connectionist networks: the sequential learning problem”. In: *Psychology of Learning and Motivation* 24.C, pp. 109–165. DOI: 10.1016/S0079-7421(08)60536-8.
- Mirzadeh, S. I., Farajtabar, M., Pascanu, R., and Ghasemzadeh, H. (2020). “Understanding the role of training regimes in continual learning”. In: *Advances in Neural Information Processing Systems*. Vol. 34.
- Niv, Y. (2021). “The primacy of behavioral research for understanding the brain”. In: *Behavioral Neuroscience* 135.5, pp. 601–609. DOI: 10.1037/bne0000471.

- Parisi, G. I., Kemker, R., Part, J. L., Kanan, C., and Wermter, S. (2019). “Continual lifelong learning with neural networks: a review”. In: *Neural Networks* 113, pp. 54–71. DOI: 10.1016/j.neunet.2019.01.012.
- Poggio, T., Fahle, M., and Edelman, S. (1992). “Fast perceptual learning in visual hyperacuity”. In: *Science* 256.5059, pp. 1018–1021. DOI: 10.1126/science.1589770.
- Ramasesh, V. V., Dyer, E., and Raghu, M. (2020). *Anatomy of catastrophic forgetting: hidden representations and task semantics*. arXiv: 2007.07400 [cs.LG].
- Ratcliff, R. (1990). “Connectionist models of recognition memory: constraints imposed by learning and forgetting functions”. In: *Psychological Review* 97.2, pp. 285–308. DOI: 10.1037/0033-295X.97.2.285.
- Ritter, H., Botev, A., and Barber, D. (2018). “A scalable laplace approximation for neural networks”. In: *6th International Conference on Learning Representations, ICLR 2018, Conference Track Proceedings*.
- Robins, A. (1995). “Catastrophic forgetting, rehearsal and pseudorehearsal”. In: *Connection Science* 7.2, pp. 123–146. DOI: 10.1080/09540099550039318.
- Schoups, A., Vogels, R., Qian, N., and Orban, G. (2001). “Practising orientation identification improves orientation coding in V1 neurons”. In: *Nature* 412.6846, pp. 549–553. DOI: 10.1038/35087601.
- Sutton, R. S. (1986). “Two problems with backpropagation and other steepest-descent learning procedures for networks”. In: *Proceedings of the 8th Annual Conference of the Cognitive Science Society*, pp. 823–831.
- Zenke, F., Poole, B., and Ganguli, S. (2017). “Continual learning through synaptic intelligence”. In: *Proceedings of the 34th International Conference on Machine Learning*. Vol. 70, pp. 3987–3995.

A Curricula category parameters

Task parameters for both curricula in experiment 1 can be found in table 1. Each task is a binary classification of two 2D Gaussian categories, with μ and v as mean vectors for each category distribution. All categories have covariance $\sigma^2 I$ with $\sigma^2 = 0.05$.

Table 2 details task parameters for each random curriculum in experiments 2 and 3. In experiment 2, the first task is always equal to the first task of curriculum 0. In experiment 3, both first and second task parameters are as described in the table.

Table 3 details digit pairings for each random split-MNIST curriculum in experiment 4.

B Effect of learning rate

In the main text learning rate is fixed at 0.001. Here, we present a supplementary analysis of different choices of learning rate on our principal results from experiment 3. Figure 1a shows the first and second task validation loss after training on each task, indicating that the task is not successfully learned for learning rates $\leq 1 \times 10^{-5}$. For all other learning rates $> 1 \times 10^{-5}$, fig. 1b outlines a clear positive trend: a larger learning rate leads to a larger number of curricula exhibiting forgetting. Figure 1c confirms that our max-norm heuristic remains highly-significantly and strongly positively-correlated ($p < .001$) with future catastrophic forgetting in all cases where the tasks have successfully been learned, i.e. $LR > 1 \times 10^{-5}$.

C Effect of weight decay

Similarly, while our primary experiments do not use weight decay, we here present a supplementary analysis of the effect of weight decay on experiment 3. From fig. 2a we see that all models trained with all weight decay settings < 1.0 successfully learn the task. In fig. 2b we observe broadly similar numbers of curricula that induce forgetting across models trained on all weight decay values, with an exception for a weight decay of 1.0, where low incidence of CF is best explained by poor performance on the first task even before moving to the second. We also confirm, in fig. 2c, that the max-norm heuristic remains significantly correlated ($p < .001$) with CF in all scenarios where the first task has been successfully learned.

D Effect of task distance

In our final supplementary analysis, we evaluate the effect of task distance, γ , i.e. a scalar controlling the similarity of two tasks within a curriculum. Figure 3a shows that task distance has no effect on the ability of the models to learn both first and second task in experiment 3. Interestingly, fig. 3b suggests that both decreasing and increasing task distance may decrease incidence of CF, though an “in-between” task distance (around $\gamma = 0.25$ as used in the main

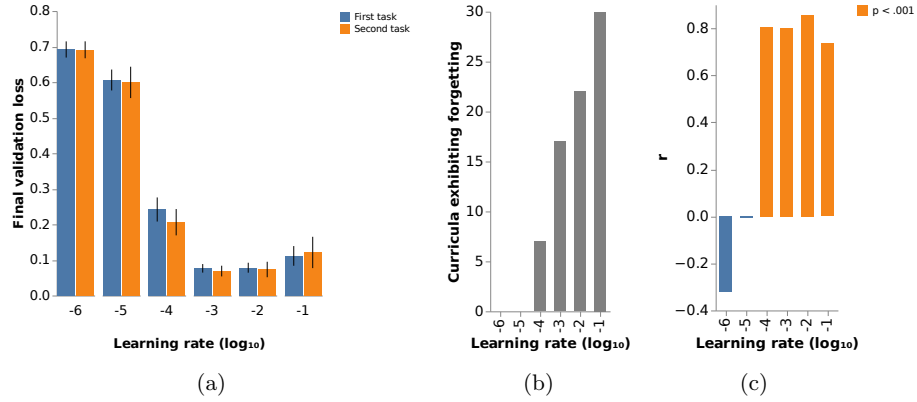


Figure 1: **Experiment 3:** (a) Final validation loss on each task by learning rate. (b) Number of curricula exhibiting forgetting by learning rate. (c) Pearson correlation of change in first task loss and max-norm of first gradient update, by learning rate.

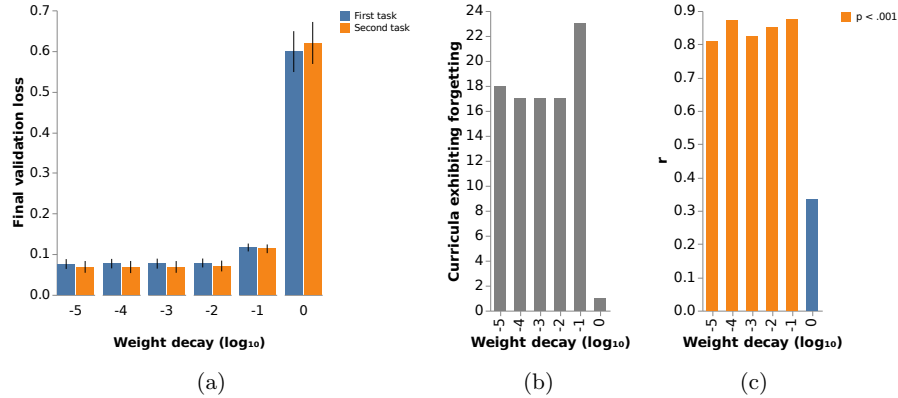


Figure 2: **Experiment 3:** (a) Final validation loss on each task by weight decay. (b) Number of curricula exhibiting forgetting by weight decay. (c) Pearson correlation of change in first task loss and max-norm of first gradient update, by weight decay.

text) is associated with the most CF. Finally, we note in fig. 3c that the max-norm heuristic is also strongly and significantly correlated ($p < .001$) in all cases except for largest task distance evaluated here, $\gamma = 0.35$, which remains positively correlated and significant, though at a lower threshold after correction for multiple comparison ($r = 0.576, p = .005$).

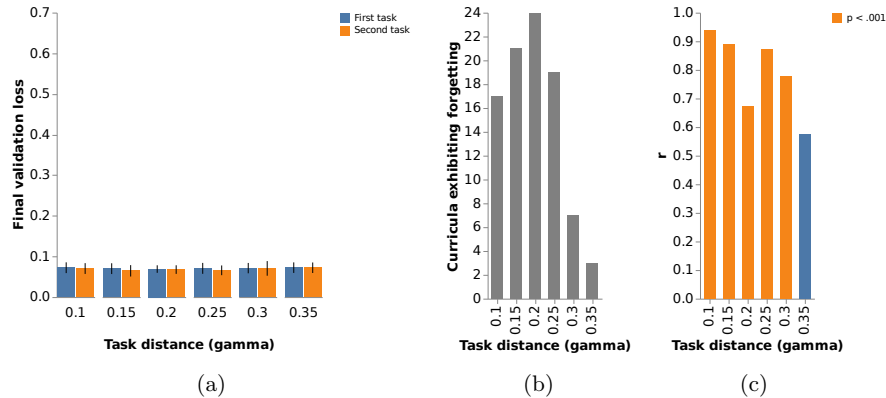


Figure 3: **Experiment 3:** (a) Final validation loss on each task by task distance, γ . (b) Number of curricula exhibiting forgetting by task distance. (c) Pearson correlation of change in first task loss and max-norm of first gradient update, by task distance.

Curriculum	Task 1		Task 2				Task 3					
	μ_0	μ_1	v_0	v_1	μ_0	μ_1	v_0	v_1	μ_0	μ_1	v_0	v_1
S	0.1	0.5	0.3	0.5	0.4	0.5	0.6	0.5	0.7	0.5	0.9	0.5
P	0.4	0.2	0.6	0.2	0.4	0.4	0.6	0.4	0.4	0.6	0.6	0.6

Table 1: **Experiment 1:** Distribution parameters for category 1 (μ) and 2 (v) for each task in \mathcal{C}_S and \mathcal{C}_P . Subscript 0 is spatial frequency; subscript 1 is orientation.

Curriculum	Task 1				Task 2			
	μ_0	μ_1	ν_0	ν_1	μ_0	μ_1	ν_0	ν_1
0	0.321	0.339	0.521	0.339	0.560	0.267	0.760	0.267
1	0.236	0.614	0.436	0.614	0.410	0.435	0.610	0.435
2	0.303	0.768	0.503	0.768	0.249	0.524	0.449	0.524
3	0.363	0.204	0.563	0.204	0.469	0.431	0.669	0.431
4	0.246	0.615	0.446	0.615	0.477	0.520	0.677	0.520
5	0.558	0.642	0.758	0.642	0.346	0.509	0.546	0.509
6	0.278	0.743	0.478	0.743	0.461	0.572	0.661	0.572
7	0.363	0.238	0.563	0.238	0.315	0.483	0.515	0.483
8	0.598	0.556	0.798	0.556	0.411	0.722	0.611	0.722
9	0.439	0.408	0.639	0.408	0.268	0.591	0.468	0.591
10	0.387	0.478	0.587	0.478	0.456	0.238	0.656	0.238
11	0.506	0.301	0.706	0.301	0.256	0.300	0.456	0.300
12	0.212	0.439	0.412	0.439	0.306	0.671	0.506	0.671
13	0.328	0.330	0.528	0.330	0.521	0.489	0.721	0.489
14	0.386	0.661	0.586	0.661	0.319	0.420	0.519	0.420
15	0.446	0.510	0.646	0.510	0.340	0.283	0.540	0.283
16	0.299	0.544	0.499	0.544	0.545	0.502	0.745	0.502
17	0.525	0.456	0.725	0.456	0.444	0.219	0.644	0.219
18	0.379	0.777	0.579	0.777	0.584	0.634	0.784	0.634
19	0.432	0.240	0.632	0.240	0.226	0.381	0.426	0.381
20	0.309	0.395	0.509	0.395	0.217	0.627	0.417	0.627
21	0.237	0.725	0.437	0.725	0.448	0.591	0.648	0.591
22	0.545	0.269	0.745	0.269	0.351	0.426	0.551	0.426
23	0.211	0.529	0.411	0.529	0.408	0.683	0.608	0.683
24	0.405	0.452	0.605	0.452	0.436	0.700	0.636	0.700
25	0.443	0.675	0.643	0.675	0.229	0.547	0.429	0.547
26	0.273	0.538	0.473	0.538	0.522	0.525	0.722	0.525
27	0.339	0.510	0.539	0.510	0.353	0.260	0.553	0.260
28	0.473	0.687	0.673	0.687	0.466	0.437	0.666	0.437
29	0.475	0.694	0.675	0.694	0.536	0.451	0.736	0.451

Table 2: **Experiments 2 and 3:** Distribution parameters for category 1 (μ) and 2 (ν) for both tasks in each randomised grating classification curriculum. Subscript 0 is spatial frequency; subscript 1 is orientation.

Curriculum	Task 1		Task 2	
	y_0	y_1	y_0	y_1
0	3	7	6	1
1	3	5	2	1
2	2	6	4	0
3	3	0	1	6
4	4	6	2	1
5	8	5	0	3
6	2	6	0	4
7	7	0	4	2
8	2	6	7	4
9	3	5	9	1
10	8	0	7	4
11	7	8	9	0
12	9	3	6	4
13	0	5	9	8
14	1	3	7	0
15	5	9	2	3
16	8	5	4	3
17	5	7	3	3
18	2	1	3	0
19	4	0	8	6
20	3	2	9	1
21	3	7	1	2
22	9	0	4	2
23	7	5	9	4
24	5	5	9	1
25	3	7	5	0
26	4	0	8	9
27	5	0	4	7
28	8	4	6	5
29	0	8	4	2

Table 3: **Experiments 4:** Selected digit pairs (y_0, y_1) for both tasks in each randomised split MNIST classification curriculum.